

Combining core floods and numerical simulation to measure flow properties in heterogeneous rocks

Samuel Krevor, Simeon Agada, Sam Jackson, Catriona Reynolds, Ben Niu
Department of Earth Science & Engineering, Imperial College London, London, United Kingdom

This paper was prepared for presentation at the International Symposium of the Society of Core Analysts held in Vienna, Austria, 27 August – 1 September 2017

ABSTRACT

This paper develops the combined use of numerical simulation with core analysis to account for the impact of multi scale rock heterogeneity on equivalent relative permeability. In this workflow laboratory measurements that are a variation of conventional SCAL tests are used to derive properties for the parameterisation of an accurate digital rock model for simulation. An equivalent relative permeability at the range of capillary numbers relevant to flow in the reservoir is derived from numerical simulations of core floods that include capillary pressure heterogeneity. We present results in which digital rock models have been developed alongside core flood observations for three applications: (1) A Bentheimer sandstone with a simple axial heterogeneity to demonstrate the validity and limitations of the approach, (2) a reservoir rock from the Bunter sandstone in the UK North Sea targeted for CO₂ storage, and (3) a Berea sandstone with small layered heterogeneities for which a CO₂-EOR coreflooding program is planned. There are layered heterogeneities present in each rock ranging from multi-cm scale for the Bentheimer to mm-scale for the Berea sandstone. Simulation results on the Bentheimer and Bunter sandstone models show that equivalent relative permeability at low flow rates will be lower than viscous limit relative permeability by a factor of 5.

INTRODUCTION

Understanding the flow of multiple fluid phases in the subsurface has been of significant interest to scientists and engineers working in petroleum and groundwater hydrology for over a century. A key component in the analysis of these flows involves sampling rocks from the subsurface and characterising their flow properties. For single phase flow, this involves the analysis of porosity and absolute permeability. When multiple fluid phases are involved, capillary pressure and relative permeability characteristics are also characterised. The multiphase flow properties depend on the fractional pore occupancy of the fluid phases, i.e. the saturation, and hysteresis in the property-saturation relationships are sometimes also evaluated, along with the irreducible, or residual, saturations of each of the fluid phases.

Rock samples obtained from subsurface wells provide some of the most detailed information about the petrophysics of the reservoir. At the same time, there are a number

of practical issues which limit the nature of subsurface samples that can be analysed: (1) Rock samples obtained from wells (rock cores) are small. Conventional rock samples are 10-13cm in diameter. (2) The size scale of samples is also limited by size scales that can be practically evaluated in the laboratory setting. The length of the rock cores can vary, but it is rare to evaluate rock cores of a meter in length in the laboratory, although it is possible to acquire such cores from the field.

The theoretical justification for the use of flow properties derived from rock core analysis is based in Effective Medium Theory. See *Renard and de Marsily (1997)* [1] and more recently *Ringrose and Bentley (2015)* [2] for reviews. There is a prescription inherent in this that measurements of properties be made in a representative elementary volume of material. In the presence of heterogeneity, however, effective multiphase flow properties cannot be obtained [1]. This basis thus requires that laboratory observations of multiphase flow properties be obtained from homogenous and isotropic rock samples. Even in the context of this theoretical construct, the size of the representative elementary volume for multiphase flow properties is unclear [3]. It may be larger than samples that are readily obtained or practically used in the laboratory.

A number of studies have shown how saturation heterogeneity, and thus relative permeability heterogeneity, will arise in rocks with small variations in capillary pressure characteristics [4-7]. This is particularly true for flow conditions relevant to those of the reservoir system. In reservoir systems, typically low flow rates will allow for capillary redistribution to control fluid saturations over the centimeter length scales at which laboratory measurements are made. Thus, even rock cores which have been identified as homogenous by single phase tracer tests are unlikely to be so at conditions relevant to the reservoir system [7]. By extension a relative permeability curve obtained at high flow rates in the laboratory such that a homogenous saturation distribution can be obtained will have little relevance or predictive value for describing flow in the reservoir system.

The remaining alternative is to derive *equivalent* properties on the naturally heterogeneous samples. This term is typically reserved for flow properties obtained from observations where flow through the sample experiences and is affected by heterogeneity in the same manner as it would in the reservoir [1]. The derivation of relevant equivalent properties, however, also places severe demands on the observation - flow rates, fluids and fluid properties, and the orientation of rock heterogeneity with respect to flow must all be as they are experienced in the reservoir. This set of constraints has been seen to be insurmountable, and no attempts have been made to develop a protocol for measuring properties on heterogeneous rocks. Despite the clear violation of theoretical assumptions, the general protocol remains to perform multiphase flow property measurements at high fluid flow rates in the most homogenous rock cores that can be obtained.

In this work we show that advances in both observational and modeling techniques can be combined to overcome the problems associated with measuring equivalent properties on heterogeneous rocks. Recent work has demonstrated that fluid saturation heterogeneity

observed in rock cores using X-ray imaging can be used as a sensitive measure to characterise capillary pressure heterogeneity [5-8]. This is the principal heterogeneity of interest for characterising multiphase flow. We build on those approaches and combine this with recent developed modeling techniques, primarily those of *Krause et al. (2013)* [6], to build a numerical representation of the rock core. The salient heterogeneous features included in the models are principally heterogeneity in the capillary pressure characteristic curves.

It is the digital model that is used to derive the relevant equivalent relative permeability curve. This digitally derived relative permeability is the one to be used as the basis for upscaling and field scale reservoir simulation. An accurate digital model can generate this information at flow rates and simulating fluids that were not necessarily the ones used in the observation. There is also some ability to reorient the rock core with respect to the fluid flow direction. In this paradigm, the goal of the observations also shifts. Conventionally the focus of observations is on obtaining the most accurate relative permeability curve directly from the observations, often with a simulated based history match of the data. In the approach presented here, the goal becomes to parameterise the numerical model with the highest degree of accuracy.

MATERIALS AND METHODS

We developed the approach using observations made on three sandstone rock cores, a Bentheimer sandstone with a simple heterogeneity parallel to the axis of flow and described in *Reynolds and Krevor (2015)* [7], a rock core from the Bunter sandstone of the Southern North Sea of the UK [8], and a Berea sandstone rock core with parallel bedding. The rock cores were cut to 3.81 cm (1.5 inches) in diameter. The length, permeability, porosity, and capillary pressure characteristics for the rocks are provided in Table 1. The average porosity along the length of each rock core is shown in Figure 1.

The Bentheimer sandstone is a shallow marine sandstone which forms the unit for oil reservoirs in the Netherlands and Germany. It is frequently used in petrophysical studies due to its availability in quarries, high permeability, and homogeneity. The sample used was 95% fine to medium grained quartz with minor feldspar, and clay with a well sorted grain size distribution.

The Bunter sandstone sample was a medium-grained sandstone composed mainly of sub-angular to sub-rounded quartz grains with a minor component of detrital K-feldspar, clay, and carbonate clasts with a well sorted grain size distribution. The core sample was obtained from the British Geological Survey Core Store. It was derived from the Cleethorpes-1 well at 1312 m depth. This was a geothermal borehole located just onshore near the town of Cleethorpes in North East Lincolnshire, UK. Further details about the rock and experimental observations can be found in *Reynolds, (2016)* [8].

The Berea sandstone was an outcrop rock from the United States and is widely used in studies as a benchmark for petrophysical work [12]. The sample was heated above 700C for over 4 hours to stabilise kaolinite clay.

Observations were chosen to parameterise the numerical model accurately with the minimum number of observations. The following formed the principle observations: average absolute permeability, porosity, relative permeability in the viscous flow limit (high flow velocities), and heterogeneous saturation maps of the rock core at a wide range of average saturations. Relative permeability data was obtained by performing steady state relative permeability experiments using an approach described in detail in *Reynolds and Krevor (2015)* [7,8]. Saturation maps were obtained during various fractional flow steps of the steady state relative permeability tests.

In the Bentheimer sandstone, observations were made during primary drainage with nitrogen and water at 50°C and 15.5 MPa pore pressure. The total fluid flow rate of the viscous limit relative permeability observation was $Q_T = Q_{N_2} + Q_{water} = 40 \text{ ml min}^{-1}$. Equivalent relative permeability was simulated at $Q_T = 7 \text{ ml min}^{-1}$. In the Bunter sandstone, observations were made during primary drainage with a CO₂-brine (1M NaCl) system at 53°C and 13.1 MPa pore pressure. The viscous limit relative permeability was obtained at $Q_T = 20 \text{ ml min}^{-1}$. Equivalent relative permeability was simulated at $Q_T = 0.2 \text{ ml min}^{-1}$. Observations in the Berea sandstone were obtained during primary imbibition using N₂ and water at 22°C and 10 MPa. The experimental flow rate was $Q_T = 20 \text{ ml min}^{-1}$. Simulations have not been completed for the Berea sandstone. In all cases, the capillary pressures that can be obtained in laboratory core floods with low viscosity fluids are limited, and the use of nitrogen also limits the possibility of making observations at high non-wetting phase saturation [12].

Saturation maps were used to characterise the capillary heterogeneity [5,9]. The saturation, including the 3D saturation maps were obtained using an X-ray CT scanner during the flow experiments. For the 3D saturation maps, scans were repeated three times at each step. Averaging imagery over multiple scans allows for a boost in precision in the X-ray imagery which is affected by significant, but random, noise.

A capillary pressure curve derived from mercury porosimetry was assumed to represent the upscaled character of the rock core (Figure 2). During a flow experiment, initially it was assumed that the capillary pressure was constant at a given location along the axis of flow, i.e., that each “slice” of the core had a constant capillary pressure. The average saturation in the slice of the rock core was assumed to map to the capillary pressure obtained from the mercury porosimetry experiment. Thus, the range of saturation in a given slice was indicative of the heterogeneity in the capillary pressure characteristic curve functions for that slice. This is similar to the initial guess used by *Krause et al. (2013)* [6]. In this work, we use simple vertical scaling to vary the capillary pressure characteristic curves,

$$P_c(x, y, z, S) = \kappa(x, y, z)P_{c,a}(S) \quad (1)$$

where $P_{c,a}$ is the average characteristic curve, a function of saturation, and P_c is the curve for a given location and saturation. These are related to the average through the location-specific scaling parameter, κ . The scaling parameter is initially obtained from the experimental data following the approach of *Pini and Benson (2013)* [9]. This extended the whole-core technique developed by *Lenormand and Eisenzimmer (1993)* [10] to millimetre scale capillary pressure characteristics.

In fitting curves for a given location, the slice averaged saturation (average at a given axial location) was mapped to the capillary pressure using the curves derived from mercury porosimetry. One point on the capillary pressure-saturation relationship was obtained for each fractional flow of the experiment. This was used to construct a capillary pressure dataset for a given location. The core representative capillary pressure curve (from mercury porosimetry) was then scaled by varying the entry pressure (Equation 1) in a regression algorithm until a best fit was obtained for the location.

The assumption of constant capillary pressure at a given location along the axis of flow, however, appears to be valid only at the inlet face of the rock core [6]. Here it is a boundary condition imposed by the experimental apparatus [10,11]. In *Krause et al. (2013)* [6] this assumption was relaxed through an iterative process - capillary pressure characteristic curves in a simulation grid block were updated until local saturations matched the experiment. The parameter was subsequently varied during the matching process to obtain a best fit of saturation. In the matching of saturation data beyond the initial guess, we stretched the distribution of scaling factors, κ , by increasing the variance in the distribution, while preserving the order of scaling factors throughout the domain of the rock model.

We represent the rock core using a model grid with grid cells the same dimension as the voxels obtained from the experimental observations, resulting in a grid of $16 \times 16 \times 40$. In this way, a direct location-specific comparison could be made between the observations and simulations. The ECLIPSE 100 simulator was used. The inlet and outlet boundaries were represented with a slice of grid cells with high permeability and no capillary pressure. The absolute and relative permeability for each grid cell was set to that observed in the experiments with flow rates in the viscous limit. The capillary pressure characteristic curve for each cell was set using vertical scaling. The base capillary pressure curve used a table of values from the mercury porosimetry data, converted to approximate a nitrogen-water system using the standard technique of scaling based on the respective interfacial tensions.

RESULTS

The relative permeability data and best fit curves are shown in Figure 3. The saturation range observed in the experiments was from 20 - 70% non-wetting phase (either nitrogen or CO₂) saturation. In the cases of the Bentheimer and Bunter sandstones, the relative

permeability to nitrogen remained $k_r < 0.12$ across this range. This is typical of coreflood experiments using low viscosity fluids where the maximum capillary pressure achievable is limited by the viscous pressure variation between the upstream and downstream ends of the rock core, i.e., saturation and relative permeability approaching the capillary endpoints are not approached [12]. Relative permeability of the Berea sandstone is far to the right of the saturation axis relative to the Bentheimer and Bunter sandstone data. This is due to either or both the differences in heterogeneity between the Berea and other sandstones, and the difference in displacement process. Relative permeability for the Bentheimer and Bunter sandstones were obtained during primary drainage. Relative permeability for the Berea sandstone was measured during primary imbibition, corresponding to the water-flood stage of an oil recovery process.

The heterogeneity in the capillary pressure characteristic curves are visualised with three-dimensional maps of the scaling parameter, κ , in Figure 4. A principle layering parallel to the long axis of the Bentheimer sandstone is apparent and most prominent at the downstream end of the rock core. Only a single layer can be seen indicating that the size scale associated with layering is larger than the diameter of the rock core. In the Bunter sandstone, there were repeated layers oblique to the long axis, some of which pinched out against the confining sleeve holding the rock core. The spacing between the layers was of similar dimension as the diameter of the rock core itself, i.e., 1-3 cm. Layering parallel to the axis of the rock core is evident in the Berea sandstone. The distance between these layers is far less than that of the Bentheimer and Bunter sandstones, around 5mm. The contrast in capillary characteristics was greater in the Bunter than in the Bentheimer sandstone, but greatest in the Berea sandstone.

A 2D saturation map of a central cross section of the Bentheimer sandstone is shown at steady state for a fractional flow $f_{N_2} = 0.4$ in the top panel of Figure 5. The prominent single layer is manifest most clearly in the saturation distribution at the downstream end of the rock core. There also appears to be a gravitational effect at the inlet of the core, with a high nitrogen saturation in the uppermost part of the rock core which is subsequently distributed by capillarity about halfway through the rock core.

The central and lower panel of Figure 5 show the saturation map of the same cross section in the 3D simulation based on the heterogeneity model shown in Figure 4. The central panel shows the distribution with the first guess in capillary heterogeneity and the lower panel shows the simulation results when the variance of the κ distribution is scaled by a factor of 1.2. In both cases the layer is prominent and as with the experimental observation, more clearly defined towards the downstream end of the rock core. The simulation, however, does not appear to capture the gravitational effect at the inlet of the rock core, and is likely due to the boundary condition imposed in the simulation (constant injection, evenly distributed throughout the inlet boundary grid blocks). The simulation with the scaled variance in the κ distribution has a better fit to the observations than the initial unscaled input.

Figure 6 shows the 2D saturation maps of the observed and simulated coreflood for the Bunter sandstone for a fractional flow $f_{CO_2} = 0.63$. The observations at the central and downstream ends of the rock core are well matched in the simulations. However, a region of prominent high CO_2 saturation at the upstream end of the observed core flood is not matched in the simulations. Additionally, there is a stronger capillary end effect apparent in the downstream end of the observed coreflood than in the simulations.

The impact of heterogeneity is evident in comparing the calculated equivalent relative permeabilities with the viscous limit relative permeabilities used as input into the numerical simulations (Figure 7). In both cases, the equivalent relative permeability is lower by approximately a factor of 5 than the viscous limit permeability, indicating a less efficient flux of fluid through the rock core due to the impact of capillary heterogeneity.

CONCLUSION

A workflow has been demonstrated for the use of heterogeneous rock cores in reservoir characterisation of multiphase flow properties. The workflow involves the use of corefloods with 3D saturation imaging as the basis for parameterising detailed numerical models of the rock cores. These models can then be used to derive equivalent relative permeability functions at the flow rates or other reservoir conditions of interest for reservoir modelling. In this work three rock cores with different length scales of layered heterogeneities were used in steady state core flood experiments of relative permeability. The saturation maps from the experiments were used to generate 3D models of capillary heterogeneity in the rock cores. Equivalent relative permeabilities derived from two of the rock cores showed that equivalent relative permeabilities are significantly lower when obtained at flow rates significantly lower than the viscous limit.

ACKNOWLEDGEMENTS

This work was supported in part by the Natural Environment Research Council grant number NE/N016173/1. The authors gratefully acknowledge funding from Statoil.

REFERENCES

1. Renard, P. and de Marsily, G. (1997), Calculating equivalent permeability: a review, *Advances in Water Resources*, 20, 5-6, 253-278
2. Ringrose, P., Bentley, M., (2015) Reservoir Model Design: A Practitioner's Guide. Springer, New York
3. Armstrong, R.A., Georgiadis, A., Ott, H., Klemin, D., Berg, S. (2014), Critical capillary number: Desaturation studied with fast X-ray computed microtomography, *Geophysical Research Letters*, 41, 55-60.
4. Ringrose, P.S., Sorbie, K.S., Corbett, P.W.M., Jensen, J.L. (1993), Immiscible flow behaviour in laminated and cross-bedded sandstones, *Journal of Petroleum Science and Engineering*, 9, 103-124.

5. Egermann, P., Lenormand, R. (2005), A New Methodology to Evaluate the Impact of Localized Heterogeneity on Petrophysical Parameters (k_r ; P_c) Applied to Carbonate Rocks, *Petrophysics*, 46, 5, 335-345.
6. Krause, M., Krevor, S., Benson, S.M. (2013), A Procedure for the Accurate Determination of Sub-Core Scale Permeability Distributions with Error Quantification, *Transport in Porous Media*, 98(3), 565-588.
7. Reynolds, C.A., and Krevor, S. C. (2015), Characterizing flow behaviour for gas injection: Relative permeability of CO₂-brine and N₂-water in heterogeneous rocks, *Water Resources Research*, 51, 12, 9464-9489.
8. Reynolds, C.A. (2016) Two-phase flow behaviour and relative permeability between CO₂ and brine in sandstones at the pore and core scales. PhD Thesis. Department of Earth Science & Engineering, Imperial College London
9. Pini, R., Benson, S.M. (2013), Simultaneous determination of capillary pressure and relative permeability curves from core-flooding experiments with various fluid pairs, *Water Resources Research*, 49, 3516-3530
10. Lenormand, R., Eisenzimmer, A. (1993) A novel method for the determination of water/oil capillary pressures of mixed wettability samples, *SCA Conference Paper Number 9322*
11. Ramakrishnan, T.S., Cappiello, A. (1991), A new technique to measure static and dynamic properties of a partially saturated porous medium, *Chemical Engineering Science*, 46, 4, 1157-1163.
12. Krevor, S., Pini, R., Zuo, L., Benson, S.M. (2012) Relative permeability and trapping of CO₂ and water in sandstone rocks at reservoir conditions, *Water Resources Research*, 48, 2

Rock	ϕ [-]	K [D]	L [m]	P_e [kPa]	λ [-]
Bentheimer	.22	1.81	.198	1.6	0.92
Bunter	.26	2.2	.151	0.95	.91
Berea	.18	.17	.204	2.5	0.67

Table 1. Properties of the rock samples

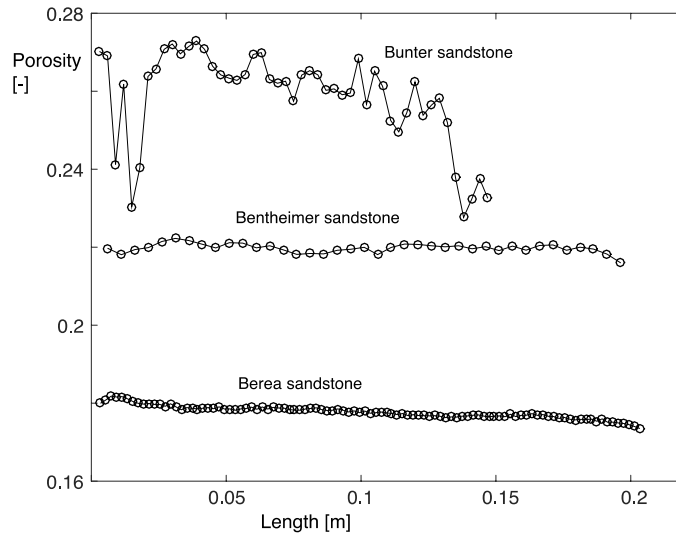


Figure 1. Average porosity along the length of the rocks for the samples investigated in this work

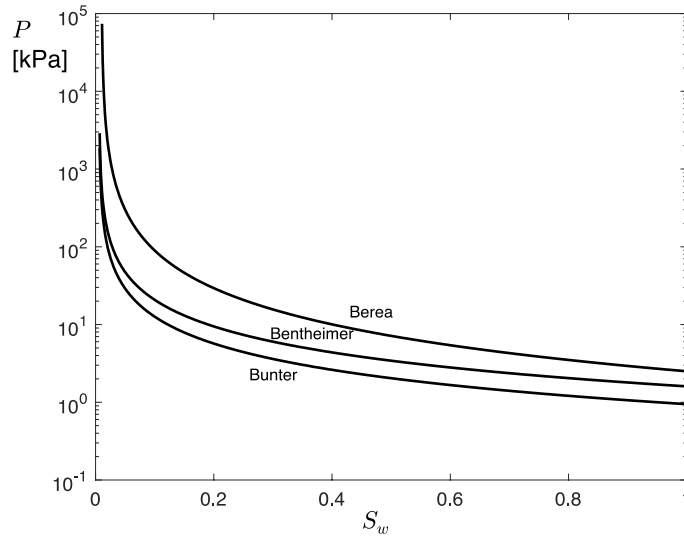


Figure 2. Best fit Brooks-Corey curves to the capillary pressure data measured using mercury porosimetry (Table 1). Saturation is normalised to the intrusion volume.

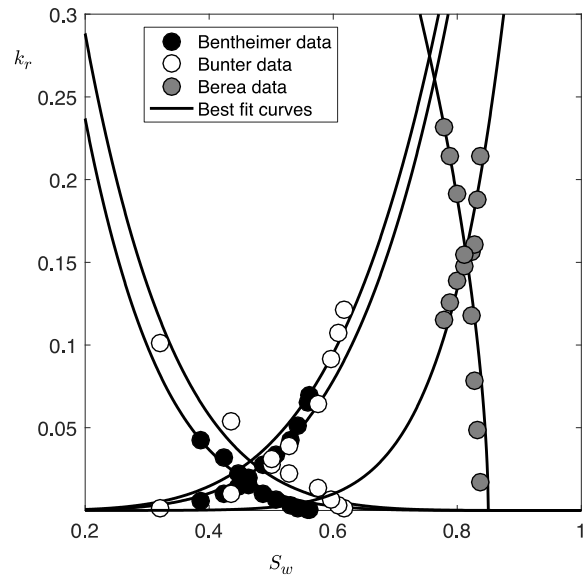


Figure 3. Relative permeability data and best fit curves for the three rocks investigated in this work. The data for the Bentheimer and Bunter sandstones are primary drainage observations. The data for the Berea sandstone is during primary imbibition

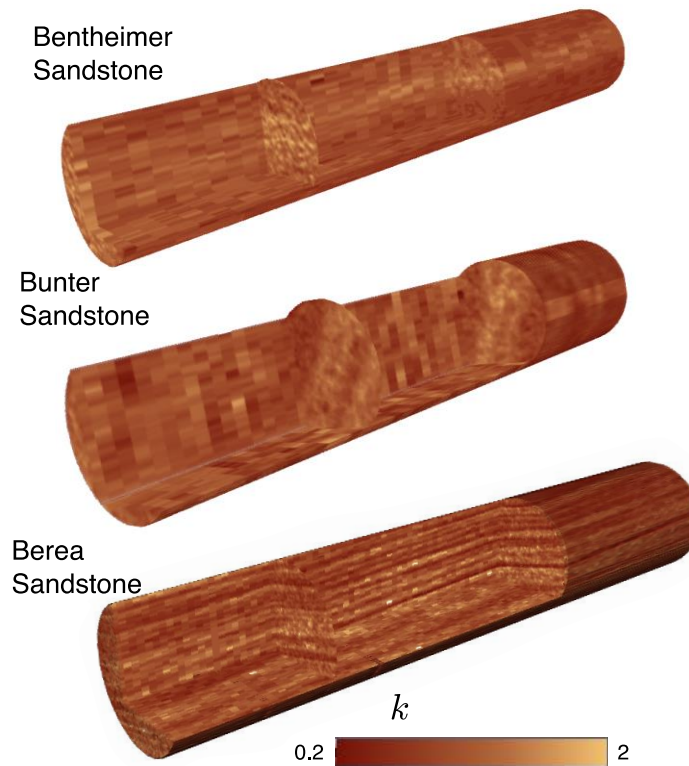


Figure 4. Rendering of the three dimensional maps of the capillary pressure scaling value, κ , for the rocks used in this study.

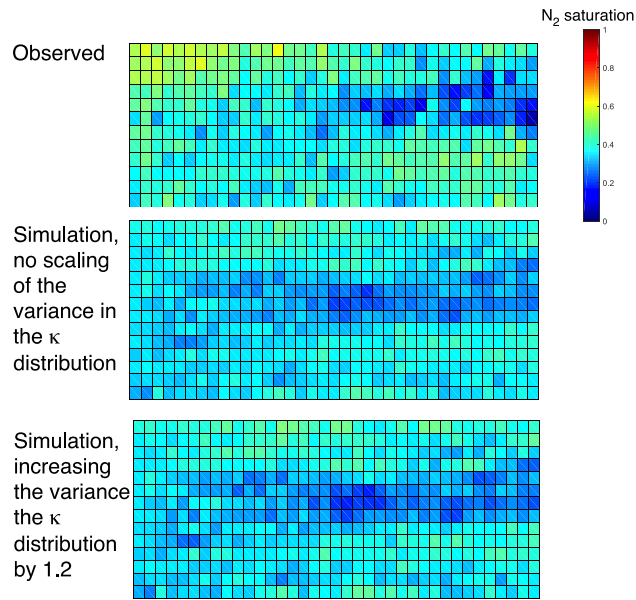


Figure 5. Experimental observations of saturation and simulated saturations in a central slice of the Bentheimer Sandstone at steady state for $f_{N_2} = 0.4$. Flow was from left to right. The vertical and horizontal lengths are shown at different scales. See Table 1 for the rock core dimensions.

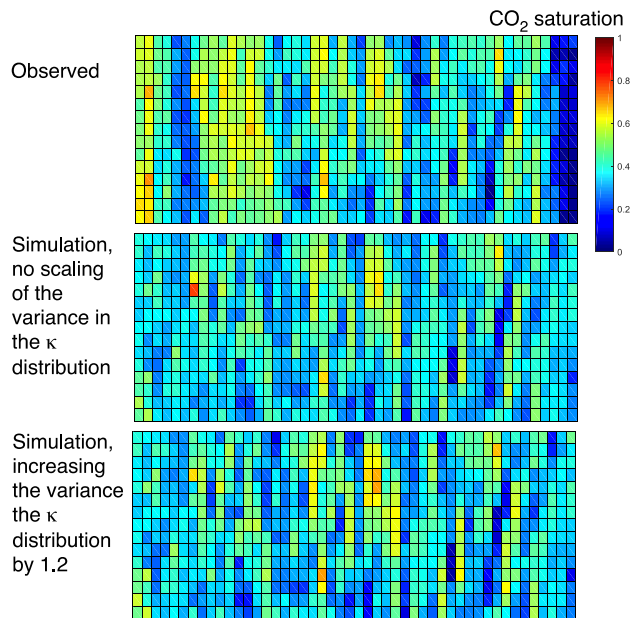


Figure 6. Experimental observations of saturation and simulated saturations in a central slice of the Bunter Sandstone at steady state for $f_{CO_2} = 0.63$. Flow was from left to right. The vertical and horizontal lengths are shown at different scales. See Table 1 for the rock core dimensions.

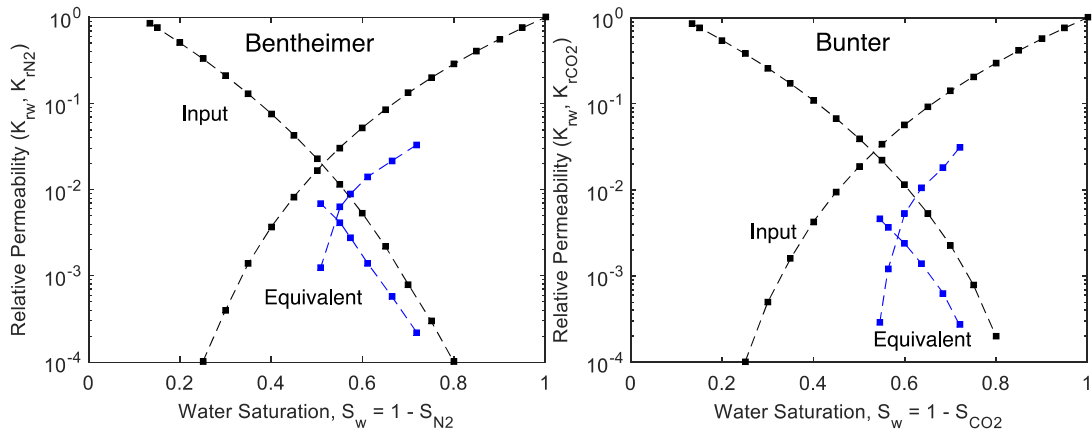


Figure 7. Input relative permeability measured in the viscous limit (in black) and simulated “synthetic” equivalent relative permeability obtained at low fluid flow velocities (blue)